

Dynamics of a large number of coupled, self-excited oscillators in a ring

Miguel A. Barron^{*1} and Mihir Sen^{**2}

**Departamento de Materiales*

Universidad Autonoma Metropolitana Azcapotzalco

Av. San Pablo 180, Col. Reynosa-Tamaulipas, Mexico, D.F., 02200 MEXICO

*** Department of Aerospace and Mechanical Engineering*

University of Notre Dame, Notre Dame, IN 46556, U.S.A.

June 17, 2011

Abstract

Interconnected, self-excited oscillators are often found in nature and in engineered devices. In this work, a ring of van der Pol oscillators, each of which is connected to its immediate neighbors, is considered. The focus is on the emergent behavior of a large number of oscillators. The conditions under which time-independent solutions are obtained are determined, and the linear stability of these solutions is investigated. The effect of the singularity of the coupling matrix on the ring dynamics is explored. When this becomes singular, an infinite number of steady states arises and the phenomenon of oscillation death is possible. Numerically-calculated dynamics of the coupled oscillators for small and large damping show complicated global behavior. Of interest are the long-time and large number of oscillators limit. It is possible to have, depending on initial conditions, all oscillators with in-phase synchrony, or metachronal traveling waves with different wavelengths going around the ring. Linear combinations, such as standing waves, are also observed. Interconnected oscillators can propagate information at a group velocity; the individual oscillators vibrate at a carrier frequency, and the signal as an amplitude modulation of that.

Keywords: Oscillation death, ring dynamics, self-excited oscillator, synchronization, van der Pol oscillator, vibration.

1 Introduction

The collective dynamics of a complex system consisting of a large number of self-excited oscillators interacting with each other in some way is very interesting. Self-excited oscillators occur in diverse fields such as biology (sleep-wake cycles [1], neurons

¹Corresponding author, e-mail: bmma@correo.azc.uam.mx

²E-mail: Mihir.Sen.1@nd.edu

[2]), optics (lasers [3]), electronics (oscillators [4]), vibrations (metronomes [5], slip-stick [6]), fluid flow (vortex shedding [7], flutter [8]), and in buildings (temperature oscillations [9]). In many cases multiple self-excited oscillators exist side by side with some interaction between them. The global behavior of the system is dependent on, but different from, that of the individual oscillators. New emergent dynamic phenomena arise when they are coupled. Frequently, however, the coupling is ignored and they are studied in isolation, so that the global dynamics is not appreciated.

The behavior of the complex system of coupled self-excited oscillators can be determined by solving the equations that govern the non-linear dynamics of each and the coupling between them. Though the details of the oscillators in each case may be different, some similarities can be observed across the board that are independent of the details of the physics behind the oscillations.

Let us start from a single self-excited oscillator governed by the autonomous equation

$$\mathcal{D}_{osc}(y) = 0, \tag{1}$$

where \mathcal{D}_{osc} is a time-independent, non-linear, differential operator that leads to self-excited oscillation. The emphasis here is on a lack of forcing by an external, periodic input which would provide a frequency; the self-excited oscillator has no need of that. Examples of such operators are integrate-and-fire [10], hysteretic thermostat [11,12], van der Pol [13], and many others. The dependent variable $y(t)$ is periodic, where t is time; it is a problem-dependent quantity that may be a current, displacement, light intensity, etc., but which will simply be referred to as motion here.

One of the simplest connection configurations possible is that of a ring [14–17]. Let us look at N of these oscillators in the form of a ring, as shown in Fig. 1, and let each be connected to its immediate neighbor on either side. The numbering system

of the ring geometry means that oscillators $i = 0$ and $i = N + 1$ are actually $i = N$ and $i = 1$, respectively. Then

$$\mathcal{D}_{osc}(y_i) = f(y_{i-1}, y_i, y_{i+1}), \quad (2)$$

with $i = 1, 2, \dots, N$, where the function f takes into account the interaction of oscillator i with its neighbors $i - 1$ and $i + 1$. Interactions between the neighbors are all of the same form.

It is intuitively obvious that it must be possible for the oscillators to move together. If all solutions of Eqs. (2) are assumed to be the same, i.e. $y_i = y(t)$, then it can be seen by substitution that it is a solution, as long as it is also assumed that $f(y, y, y) = 0$. All the oscillators move in phase, there is zero interaction, and the frequency is the same as that of a single oscillator given by Eq. (1). A numerical example for the van der Pol oscillator will be given in Section 3.2.

To be able to find other solutions, it is necessary to be more specific about the dynamics of the oscillators. Here, the specific case of van der Pol oscillators in the form of a ring with each oscillator coupled to its two nearest neighbors will be chosen. For this

$$\mathcal{D}_{osc}(y_i) = \ddot{y}_i + a(y_i^2 - 1)\dot{y}_i + y_i. \quad (3)$$

A linear difference interaction (also called diffusive [18, 19]) is given by

$$f = b(y_{i-1} - 2y_i + y_{i+1}), \quad (4)$$

so that

$$\ddot{y}_i + a(y_i^2 - 1)\dot{y}_i + y_i = b(y_{i-1} - 2y_i + y_{i+1}), \quad (5)$$

for $i = 1, 2, \dots, N$, with $a > 0$ and appropriate initial conditions.

Pioneering work on this problem was done by Linkens [14] and Endo and Mori [15]. Linkens found the analytical solution of mutually coupled identical van der Pol oscillators using the method of harmonic balance and assuming nearly sinusoidal oscillations. For nonidentical oscillators he used the Rosenbrock hill-climbing routine which yielded an acceptable solution to his algebraic model. Through a perturbation-type analysis, Endo and Mori were able to show the existence of stable traveling and standing waves of different modes. They also suggested that multimodal waves were possibly unstable, though further work was needed in this regard. Neither Linkens nor Endo and Mori performed any numerical time-integration of coupled rings. The present authors have also worked on a ring of four oscillators [13,20]. In that context they have shown that if $b < -0.25$ the oscillators are unstable [20]. Phase shift depends on the interactive coupling; as the coupling parameter is raised, the phase shift decreases, and disappears beyond a certain finite value. Others have worked on different aspects of a ring of four coupled van der Pol oscillators [21–23].

This work will build upon previous work on interacting van der Pol rings and extend them in several directions: studying the effect of singularity of the coupling matrix on the ring dynamics, consideration of a large number of oscillators, and highly non-linear behavior of the oscillator in the form of a large a . The existence and linear stability of time-independent solutions is studied in detail. Also investigated are the emergent behavior for the ring as a whole, the waves that occur, their dispersion relationship, and phase and group velocities.

2 Time-independent solutions

These are the simplest solutions to the problem; their existence and linear stability are investigated.

2.1 Existence of trivial solution

The time-independent solution of Eq. (5), indicated by an overbar, is determined from

$$b\bar{y}_{i-1} - (1 + 2b)\bar{y}_i + b\bar{y}_{i+1} = 0, \quad (6)$$

which gives $\bar{y}_i = 0$ as long as $D \neq 0$, where

$$D = \det \mathbf{B}, \quad (7a)$$

$$\mathbf{B} = \begin{bmatrix} -(1+2b) & b & 0 & \dots & 0 & b \\ b & -(1+2b) & b & \dots & 0 & 0 \\ \vdots & \vdots & \vdots & & \vdots & \vdots \\ 0 & 0 & \dots & b & -(1+2b) & b \\ b & 0 & 0 & \dots & b & -(1+2b) \end{bmatrix}. \quad (7b)$$

2.2 Linear stability of trivial solution

The linear stability of $\bar{y}_i = 0$ can be examined by perturbing it slightly and linearizing, which gives

$$\ddot{y}_i - ay_i + y_i = b(y_{i-1} - 2y_i + y_{i+1}). \quad (8)$$

This can be written as

$$\dot{y}_i = z_i, \quad (9a)$$

$$\dot{z}_i = az_i + by_{i-1} - (1 + 2b)y_i + by_{i+1}. \quad (9b)$$

In matrix form this is

$$\frac{d\mathbf{y}}{dt} = \mathbf{A}\mathbf{y}, \quad (10)$$

with

$$\mathbf{y} = [y_1 \ y_2 \ \dots \ y_N \ z_1 \ z_2 \ \dots \ z_N]^T, \quad (11)$$

$$\mathbf{A} = \begin{bmatrix} \mathbf{0} & \mathbf{I} \\ \mathbf{B} & a\mathbf{I} \end{bmatrix}, \quad (12)$$

where \mathbf{I} is the $N \times N$ identity matrix, and \mathbf{B} is given by Eq. (7b).

The $2N$ eigenvalues of the block matrix \mathbf{A} determine the stability of the time-independent solution. The characteristic polynomial of \mathbf{A} is

$$\sigma_0 \lambda^{2N} - \sigma_1 \lambda^{2N-1} + \sigma_2 \lambda^{2N-2} - \dots + (-1)^{2N} \sigma_{2N} = 0, \quad (13)$$

where

$$\sigma_0 = 1, \quad (14)$$

$$\sigma_1 = \sum_{i=1}^{2N} a_{ii} = \text{tr}(\mathbf{A}) = Na, \quad (15)$$

$$\sigma_2 = \sum_{i < j} \begin{vmatrix} a_{ii} & a_{ij} \\ a_{ji} & a_{jj} \end{vmatrix} = (N-1)a^2, \quad (16)$$

$$\sigma_3 = \sum_{i < j < k} \begin{vmatrix} a_{ii} & a_{ij} & a_{ik} \\ a_{ji} & a_{jj} & a_{jk} \\ a_{ki} & a_{kj} & a_{kk} \end{vmatrix} = (N-2)a^3, \quad (17)$$

and so forth. In addition, $\sigma_{2N} = \det \mathbf{A}$.

Polynomial stability requires that all the roots have negative real parts. The necessary and sufficient condition for this is that *all* coefficients of the first column of the Routh-Hurwitz (RH) array have the same sign. Table 1 shows the derived expressions for four coefficients of the RH array corresponding to the characteristic polynomial of Eq. (13).

The first element of the RH array is positive whereas the second one is negative. The third coefficient is always positive for any value of N . The fourth coefficient is negative for $N \geq 3$. Two sign changes are detected for these four coefficients, consequently the characteristic polynomial of \mathbf{A} has at least two right-half plane roots. This means that the RH stability condition is not satisfied and therefore the trivial solution is unstable.

2.3 \mathbf{B} singular

Since \mathbf{B} is a circulant matrix

$$D = \prod_{j=0}^{N-1} [b - (1 + 2b)e^{2\pi ij/N} + be^{4\pi ij/N}]. \quad (18)$$

The first $j = 0$ factor on the right is -1 . D can be zero if any one of the other factors vanish, i.e. if

$$b = \frac{1}{2 \{\cos(2\pi j/N) - 1\}} \quad (19)$$

for $j = 1, 2, \dots, N - 1$. Some of these critical values of b are given in Table 2, where only values that are different from each other are shown. It can be seen that for even values of N there are $N/2$ different critical values, while for odd there are $(N - 1)/2$.

An interesting behavior of coupled oscillators is amplitude death and oscillation death that occurs when they cease to oscillate [24]. Commonly, amplitude death arises through a Hopf bifurcation mechanism in coupled oscillators with an important parameter mismatch or in identical oscillators with time delays [25]. An already existing unstable steady state with zero amplitude is transformed by the coupling into a stable one allowing its observation, i.e. the coupling induces stability at the origin of the phase space. On the other hand, oscillation death occurs through a saddle-node bifurcation mechanism allowing the emergence of new fixed points: a new stable steady state with none-zero amplitude is created by the coupling [24, 25].

When \mathbf{B} is singular Eq. (6) can have an infinite number of steady-state solutions and oscillation death can arise. The right column of Table 2 shows the $\text{rank}(\mathbf{B})$ as a function of N and critical b . For even values of N , $\text{rank}(\mathbf{B}) = N - 1$ for $b = -0.25$ and $\text{rank}(\mathbf{B}) = N - 2$ for other values of b . For odd values of N , $\text{rank}(\mathbf{B}) = N - 2$, irrespective of the value of b . Then, when \mathbf{B} is singular, this matrix has one or two

linearly dependent rows or columns which can be ignored and the dynamical system can be analyzed in a reduced dimensional space.

Fig. 2 shows oscillation death for $N = 100$, $a = 0.01$, $b = -0.25$ which corresponds to \mathbf{B} singular. The initial conditions are $y_1(0) = 0.2$, $\dot{y}_1(0) = 0.2$, and $y_i(0) = \dot{y}_i(0) = 0$ for $i = 2, 3, \dots, N$. Given that N is odd, $\text{rank}(\mathbf{B}) = 99$. By fixing one of the oscillators, \mathbf{B} becomes nonsingular. This is shown in Fig. 3, where the motion of the N^{th} oscillator is fixed for $t \geq 1000$. The oscillation death state is transformed into a normal oscillatory one.

3 Waves for small a

On the contrary, if $b > -0.25$ the system exhibits stable sustained oscillations. If N is large, then the right side of Eq. (2) can be approximated by a second-order spatial derivative. Thus, writing $y_i = y(\theta_i, t)$, where θ_i is the angular position of oscillator i gives

$$y_{i-i} - 2y_i + y_{i+1} = y(\theta_{i-i}, t) - 2y(\theta_i, t) + y(\theta_{i+1}, t), \quad (20a)$$

$$\approx \frac{4\pi^2}{N^2} \frac{\partial^2 y}{\partial \theta^2}, \quad (20b)$$

where $2\pi/N$ is the angular distance between neighboring oscillators.

The nonlinear damping term $a(y^2 - 1)\dot{y}$ changes sign at $y^2 = 1$, enabling the self-excited oscillations. Assuming, for the moment, that it is small, to leading order

$$\ddot{y} + y \approx \frac{4\pi^2 b}{N^2} \frac{\partial^2 y}{\partial \theta^2}. \quad (21)$$

A solution is

$$y = A \sin(k\theta - \omega t). \quad (22)$$

Standard non-linear analysis for a single oscillator with small a gives an amplitude

of $A = 2$. This is a wave traveling in the positive θ direction of frequency ω , period $2\pi/\omega$, wave number k , and wavelength that is $(1/k)^{\text{th}}$ of the circumference of the ring.

The frequency is determined by substitution to be

$$\omega = \left(1 + \frac{4\pi^2 k^2 b}{N^2}\right)^{1/2}. \quad (23)$$

This is the dispersion relation, from which the phase velocity of the wave is found to be

$$\begin{aligned} v_p &= \frac{\omega}{k}, \\ &= \frac{1}{k} \left(1 + \frac{4\pi^2 k^2 b}{N^2}\right)^{1/2}. \end{aligned} \quad (24)$$

The group velocity is

$$\begin{aligned} v_g &= \frac{d\omega}{dk}, \\ &= \frac{4\pi^2 kb}{N^2} \left(1 + \frac{4\pi^2 k^2 b}{N^2}\right)^{-1/2}, \end{aligned} \quad (25a)$$

$$= \frac{4\pi^2 b}{N^2} \frac{1}{v_p} \quad (25b)$$

It is interesting to note that the two velocities are inversely proportional to each other, with $v_p \geq v_g$.

The individual waves travel at the phase velocity, while the information travels at the group velocity. The phase velocity decreases with the wave number k , but the group velocity increases. Furthermore, as $N \rightarrow \infty$, $v_p \rightarrow 1/k$ and $v_g \rightarrow 0$ if b is held constant. The reason for this is that the angular distance between oscillators $2\pi/N \rightarrow 0$, and hence the interaction term in Eq. (21) $4\pi^2 b/N^2 \rightarrow 0$ also. If, however, it is assumed that $b \sim N^2$ such that $4\pi^2 b/N^2 = C$, where C is a constant, then both $v_p = k^{-1}(1 + Ck^2)^{1/2}$ and $v_g = Ck(1 + Ck^2)^{-1/2}$ are independent of N . They become independent of the wave number k also for large k , and strangely enough, become equal.

Since Eq. (21) is linear, wave solutions may be superposed. This means that any initial conditions will be propagated as a wave with each constituent wave number traveling at its own phase velocity. As a special case, two waves traveling in opposite directions, i.e. with k and $-k$ in Eq. (22), may be added to give a standing wave

$$y = -2A \cos k\theta \sin \omega t. \quad (26)$$

3.1 Numerical solutions

Eqs. (5) can be solved numerically using a fourth-order Runge-Kutta method. The parameters of the system of equations are: the number of oscillators N , the nonlinear damping a , and the interaction between neighbors b . A non-zero a creates self-excitation, and no external forcing is needed, but at the same time, a small enough a satisfies the linearized analysis. Numerical solutions shown will be for $a = 0.01$, and an arbitrarily chosen $b = 1$. The time step used for integration is 10^{-4} , which is found to be small enough for numerical stability and convergence.

Specific solutions that are sought are obtained by prescribing initial conditions derived from Eqs. (22) and (26). Since the interest here is in a long-time behavior, the time after which there is no change in system response must first be found. Using Eq. (22) and its derivative as initial conditions, two numerical calculations are shown in Fig. 4(a). One is a complete period beginning after $t = 1000$, and the other begins after $t = 2000$. It is found that the solutions are converged in time, so that numerical solutions from $t = 1000$ will be sufficient. Also, for a large number of oscillators, the second step is to check for convergence with respect to N . Fig. 4(b) shows solutions for $N = 100$ and $N = 1000$, respectively, for $a = 0.01$. It is apparent that $N = 100$ is sufficiently large, and that any increase in the number of oscillators does not change the global behavior of the system.

3.2 $k = 0$

The simplest version of Eq. (22) is with zero wave number. The motion is then independent of space, and only oscillates in time. An example is shown in Fig. 5. This is full synchronization in which all oscillators move in phase. Eq. (23) shows that the frequency does not depend on N .

3.3 $k = \pm 1, \pm 2, \dots$

The temporal motions of five equally-spaced oscillators around the ring are shown in Fig. 6(a) for $k = 1$. The phases are seen to be equally spaced also. Fig. 6(b) shows three oscillators that are neighbors. The wave peaks first for $i = 40$, then $i = 41$, and finally $i = 42$, indicating a wave motion around the ring in a counter-clockwise direction. In the biological literature, especially for cilia, this is often referred to as a metachronal wave [26–28]. Similarly, there is another solution possible, $k = -1$, in which the $(i + 1)^{\text{th}}$ oscillator leads the i^{th} , so that it would be an identical wave but in the clockwise direction. These are shown in Figs. 7(a) and 7(b). Spatial variations for $k = 1$ and $k = -1$ are shown in Fig. 8 at the instant $t = 1000$. The entire ring is one wavelength of the wave.

A standing wave is formed by identical waves running in opposite directions. An example is shown in Fig. 9. Other possibilities are those of multiple integer or non-integer wavelengths in the ring depending on k . As an example, Figs. 10(a) and 10(b) show time series for $k = 2$ and $k = -2$, respectively. Fig. 11 shows the spatial variation at $t = 1000$ for these two waves.

4 Waves for large a

Van der Pol oscillators with $a \ll 1$ of Section 3 present quasilinear behavior and therefore exhibit oscillations that are nearly sinusoidal. Nonlinear behavior is more

evident for $a \geq 1$. For single van der Pol oscillators it is known that the frequency of oscillation decreases with increasing a . The form of the oscillation also changes, the rise and fall in each period becoming steeper as a increases. It is important to see the behavior of a coupled system of oscillators with large a .

The numerical results shown here are obtained in the following way. Since initial conditions have a significant effect on the long-time results, the small a initial conditions were introduced, as before. Then, however, the value of a was ramped up slowly with each time step until the desired value was reached, at which stage it was held constant for 1000 time units.

4.1 $a = 1$

Fig. 12(a) depicts a time series for $N = 100$, with initial conditions corresponding to Eqs. (22) with $k = 2$. A modulated signal is clearly visible with a dominant carrier frequency and a modulation which persists even if the integration is carried out much longer. The power spectral density, shown in Fig. 12(b), quantifies these frequencies as 0.1527 and 0.0076, respectively. The envelope is shown in further detail in Fig. 12(c) for neighboring oscillators. The envelope is itself a traveling wave that is moving at the group velocity.

4.2 $a = 10$

Figs. 13(a) and 13(b) show a time series and its corresponding power spectrum for $N = 100$ and initial conditions corresponding to $k = 2$. Three frequencies of 0.0534, 0.1607 and 0.2680 are detected. The first is the fundamental, the others being the third and the fifth harmonics, respectively. On closer examination, an interesting space-time structure is seen. The time series in Fig. 13(a) for $i = 1$ is re-drawn as Figs. 14(a), along with four other oscillators, but on a different time scale. Fig. 14(b)

is the spatial distribution at a given instant in time. Sharp leading edges are observed in both time and space.

5 Conclusions

Self-excited oscillators connected to each other in the form of a ring with linear neighbor-to-neighbor coupling have been considered. For a perfectly general nonlinear operator, it can be shown that the in-phase oscillation is a possible behavior as long as the interaction vanishes if two neighbors move together.

Global behavior of the ring was investigated by using the example of a van der Pol operator. The effect of the singularity of the coupling matrix \mathbf{B} in the ring dynamics has been explored. When this matrix becomes singular, the ring has an infinite number of steady states and oscillation death can arise. However, fixing the motion of some oscillators, the number depending on the rank deficiency of \mathbf{B} , makes the system determinate and oscillating. This can be useful for the global control of the entire ring.

For $b > 0$ and small a , it has been shown that wave-like behavior exists for different initial conditions. These dispersive, metachronal waves traveling around the ring can be analytically determined and numerically confirmed. A special case of the wave number $k = 0$ is that of complete in-phase synchronization. Other positive or negative, integer or non-integer values of k correspond to waves running in either direction around the ring. The dynamics for large a are more complicated; nonlinear behaviors, such as modulation and harmonics, emerge. Sharp temporal derivatives are well-known for single van der Pol oscillators, but it appears that connected oscillators also have a similar dynamic behavior. In addition, the spatial derivative is surprisingly similar with high spatial derivatives; neighboring oscillators exhibit extreme differences in motion as the waves pass through.

It has been shown that interconnected oscillators can propagate signals. An oscillator has an intrinsic frequency, i.e. a stand-alone frequency if it were to be completely isolated. For a van der Pol oscillator the intrinsic linear frequency for small a , determined by the coefficients of the \ddot{y} and y terms, has been taken to be unity here. However, as a becomes larger the intrinsic nonlinear frequency is somewhat smaller. For communication purposes this is a carrier frequency. Interaction between oscillators, however, is determined by the coupling constant b . For non-zero b , information travels at group velocity along the ring in the form of waves as an amplitude modulation of the carrier.

References

- [1] C. Tenreiro and R. Elgueta. Modeling the sleep-wake cycle using coupled Van der Pol oscillators. *Biological Rhythm Research*, 41(2):149–157, 2010.
- [2] K. Tsumoto, T. Yoshinaga, and H. Kawakami. Bifurcations of synchronized responses in synaptically coupled Bonhoffer-van der Pol neurons. *Physical Review E*, 65(3): Article No. 036230, Part 2A, 2002.
- [3] V. Blazek. A semiconductor laser as a classical Van der Pol oscillator controlled by an external signal. *Czechoslovak Journal of Physics*, 18(5):644–646, 1968.
- [4] A. Algaba, F. Fernandez-Sanchez, E. Freire, E. Gamero, and A.J. Rodriguez-Luis. Oscillation-sliding in a modified van der Pol-Duffing electronic oscillator. *Journal of Sound and Vibration*, 249(5):899–907, 2002.
- [5] J. Pantaleone. Synchronization of metronomes. *American Journal of Physics*, 70(10):992–1000, 2002.
- [6] A.J. McMillan. A non-linear friction model for self-excited vibrations. *Journal of Sound and Vibration*, 205(3):323–335, 1997.
- [7] P.A. Monkewitz. Modeling of self-excited wake oscillations by amplitude equations. *Experimental Thermal and Fluid Science*, 12(2):175–183, 1996.
- [8] E.H. Dowell and K.C. Hall. Modeling of fluid-structure interaction. *Annual Review of Fluid Mechanics*, 33:445–490, 2001.
- [9] R.J. Duffin and G. Knowles. A passive wall design to minimize temperature swings. *Solar Energy*, 33(3-4):337–342, 1984.
- [10] P. Goel and B. Ermentrout. Synchrony, stability, and ring patterns in pulse-coupled oscillators. *Physica D*, 163:191–216, 2002.

- [11] W. Cai, M. Sen, K.T. Yang, and R.L. McClain. Synchronization of self-sustained thermostatic oscillations in a thermal-hydraulic network. *International Journal of Heat and Mass Transfer*, 49:4444–4453, 2006.
- [12] W. Cai and M. Sen. Synchronization of thermostatically controlled first-order systems. *International Journal of Heat and Mass Transfer*, 51(11-12):3032–3043, 2008.
- [13] M.A. Barron and M. Sen. Synchronization of four coupled van der Pol oscillators. *Nonlinear Dynamics*, 56(4):357–367, 2009.
- [14] D. A. Linkens. Analytical solution of large numbers of mutually coupled nearly sinusoidal oscillators. *IEEE Transactions on Circuits and Systems*, CAS-21(2):294–300, 1974.
- [15] T. Endo and S. Mori. Mode analysis of a ring of a large number of mutually coupled Vanderpol oscillators. *IEEE Transactions on Circuits and systems*, 25(1):7–18, 1978.
- [16] J. Bridge, L. Mendelowitz, R. Rand, S. Sah, and A. Verdugo. Dynamics of a ring of three coupled relaxation oscillators. *Communications in Nonlinear Science and Numerical Simulation*, 14(4):1598–1608, 2009.
- [17] R. Yamapi, H.G.E. Kadji, and G. Filatrella. Stability of the synchronization manifold in nearest neighbor nonidentical van der Pol-like oscillators. *Nonlinear Dynamics*, 61:275–294, 2010.
- [18] A. Pogromsky and H. Nijmeijer. Cooperative oscillatory behavior of mutually coupled dynamical systems. *IEEE Transactions on Circuit and Systems–I: Fundamental Theory and Applications*, 48(2):152–162, 2001.
- [19] D.V. Senthilkumar, P. Muruganandam, M. Lakshmanan, and J. Kurths. Scaling and synchronization in a ring of diffusively coupled nonlinear oscillators. *Physical Review E*, 81: Article No. 066219, 2010.
- [20] M.A. Barron, M. Sen, and E. Corona. Dynamics of large rings of coupled Van der Pol oscillators. In K. Elleithy, editor, *Innovations and Advanced Techniques in Systems, Computing Sciences and Software Engineering*, pages 346–349. Springer, 2008.
- [21] T. Ookawara and T. Endo. Effects of the deviation of element values in a ring of three and four coupled van der Pol oscillators. *IEEE Transactions on Circuits and Systems I-Fundamental Theory and Applications*, 46:827–840, 1999.
- [22] B. Nana and P. Wofo. Synchronization in a ring of four mutually coupled van der Pol oscillators: Theory and experiment. *Physical Review E*, 74(4), Article No. 046213, 2006.
- [23] V.P. Kruglov and S.P. Kuznetsov. An autonomous system with attractor of Smale-Williams type with resonance transfer of excitation in a ring array of van der Pol oscillators. *Communications in Nonlinear Science and Numerical Simulation*, 16(8):3219–3223, 2011.

- [24] W. Zou, X. Wang, Q. Zhao, and M. Zhan. Oscillation death in coupled oscillators. *Frontiers of Physics in China*, 374:178–185, 2009.
- [25] J.J. Suarez-Vargas, J.A. Gonzalez, A. Stefanovska, and P.V.E. McClintock. Diverse routes to oscillation death in a coupled-oscillator system. *EPL*, 85:38008, 2009.
- [26] S.M. Mitran. Metachronal wave formation in a model of pulmonary cilia. *Computers and Structures*, 85:763–774, 2007.
- [27] T. Niedermayer, B. Eckhardt, and P. Lenz. Synchronization, phase locking, and metachronal wave formation in ciliary chains. *Chaos*, 18: Article No. 037128, 2008.
- [28] S. Tadokoro, Y. Yamaguti, H. Fujii, and I. Tsuda. Transitory behaviors in diffusively coupled nonlinear oscillators. *Cognitive Neurodynamics*, 5(1):1–12, 2011.

Table 1: First-column coefficients of the Routh-Hurwitz array.

Exponent of λ	Coefficient
$2N$	1
$2N - 1$	$-Na$
$2N - 2$	$\frac{a^2(N^2 - 2N + 2)}{N^2 - 2N + 2}$
$2N - 3$	$\frac{-2a^3(N - 2)}{N^2 - 2N + 2}$
\dots	\dots

Table 2: Different values of b at which $D = \det \mathbf{B}$ vanishes; rank of \mathbf{B} shown in brackets.

N	b [rank of \mathbf{B}]					
3	-0.3333 [1]					
4	-0.2500 [3]	-0.5000 [2]				
5	-0.2764 [3]	-0.7236 [3]				
6	-0.2500 [5]	-0.3333 [4]	-1.0000 [4]			
7	-0.2630 [5]	-0.4090 [5]	-1.3280 [5]			
8	-0.2500 [7]	-0.2929 [6]	-0.5000 [6]	-1.7071 [6]		
9	-0.2578 [7]	-0.3333 [7]	-0.6051 [7]	-2.1372 [7]		
10	-0.2500 [9]	-0.2764 [8]	-0.3820 [8]	-0.7236 [8]	-2.6180 [8]	

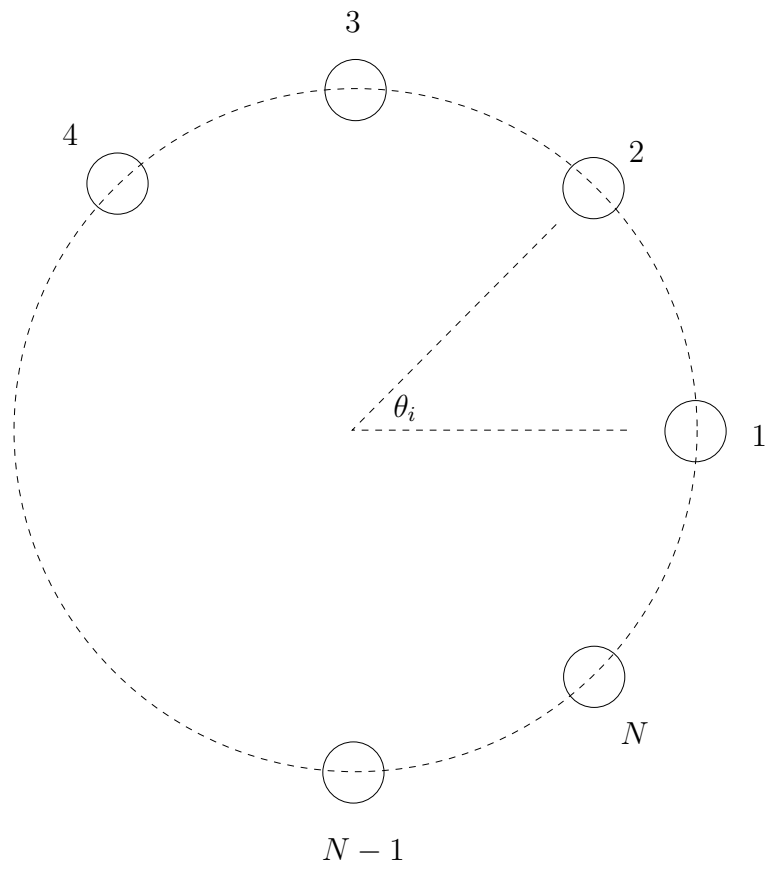


Figure 1: N self-excited oscillators in a ring.

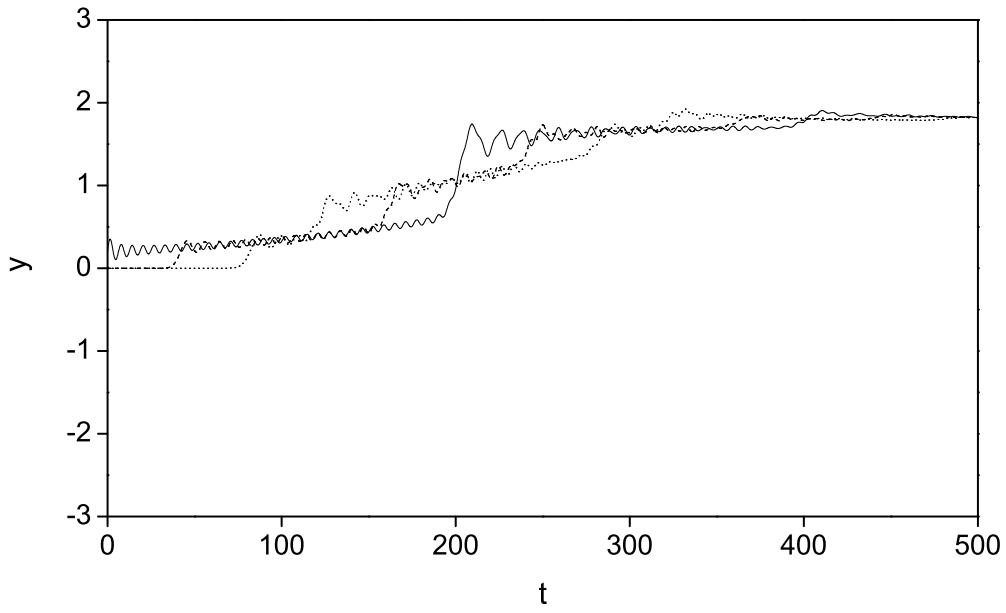


Figure 2: Oscillation death, with $N = 100$, $a = 0.01$, $b = -0.25$, $k = 2$, $y_1(0) = \dot{y}_1(0) = 0.2$, $y_i(0) = \dot{y}_i(0) = 0$ for $i = 2, \dots, N$. Lines: solid $i = 1$, dashed $i = 41$, dotted $i = 81$.

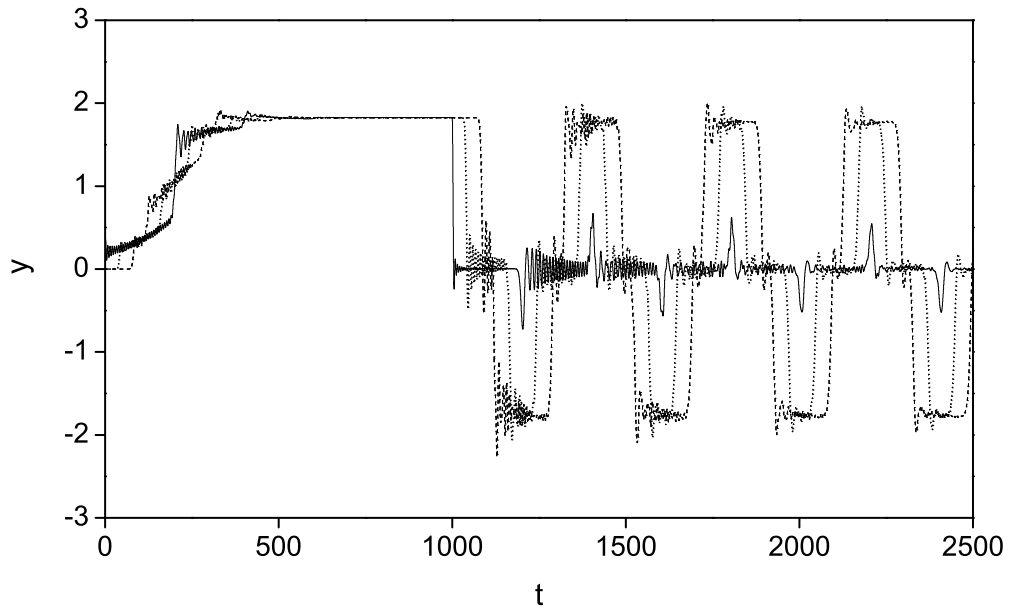
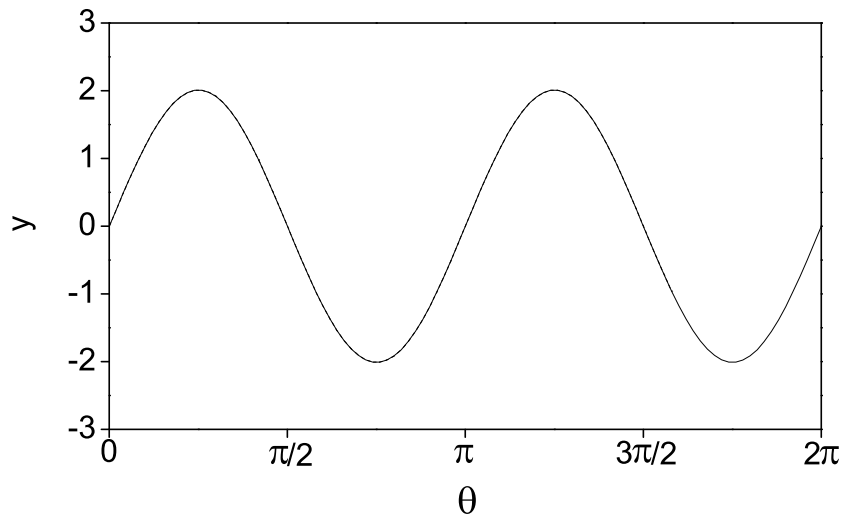
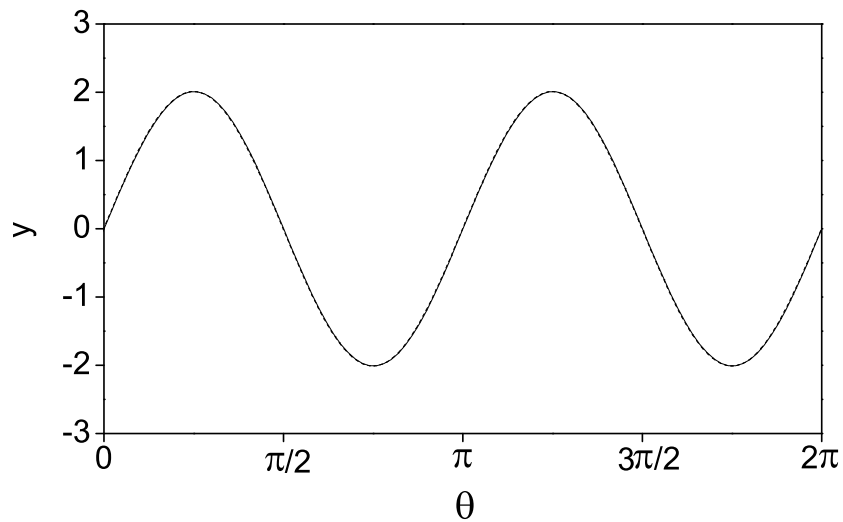


Figure 3: Disappearance of oscillation death on fixing $y_N(t) = \dot{y}_N(t) = 0$ for $t \geq 1000$. Parameters and initial conditions are the same as in Fig. 2. Lines: solid $i = 1$, dashed $i = 41$, dot $i = 81$.



(a)



(b)

Figure 4: (a) Convergence with respect to integration time, $N = 100$, $k = 2$. Lines: solid $t = 1000$, dashed $t = 2000$. (b) Convergence with respect to number of oscillators, $t = 1000$. Lines: solid $N = 100$, dashed $N = 1000$.

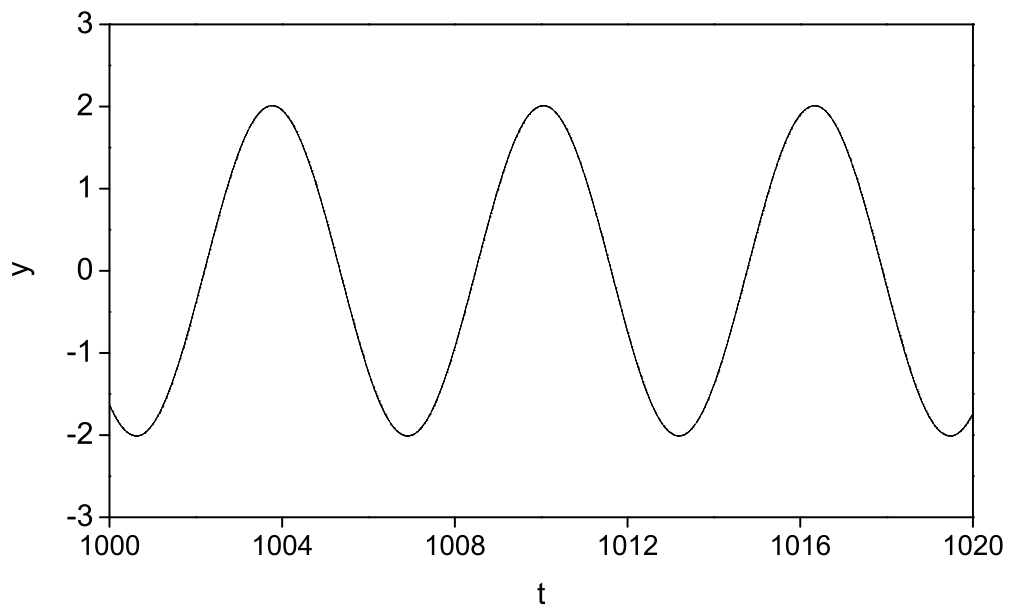
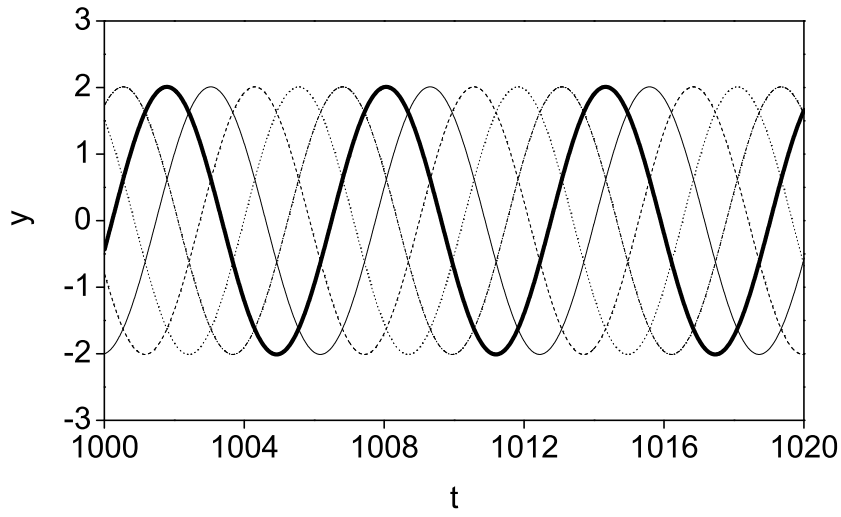
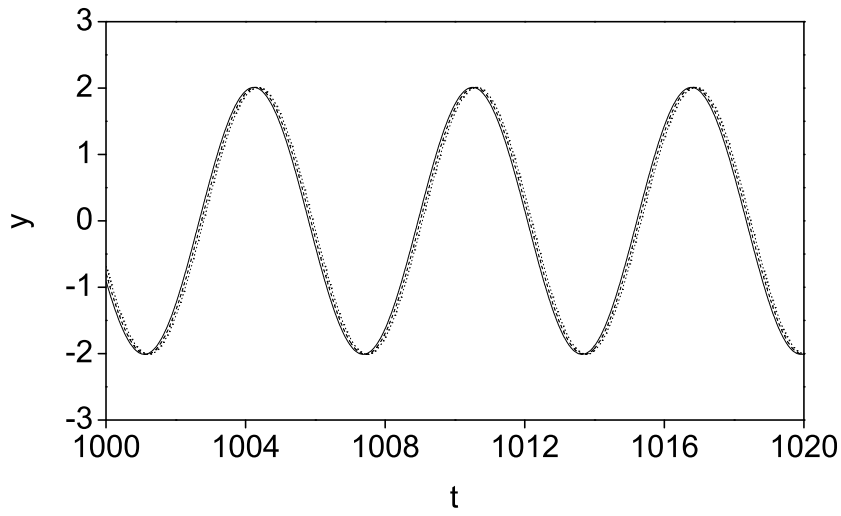


Figure 5: Time series for $k = 0$ and $i = 1, 21, 41, 61, 81$; all curves coincide.

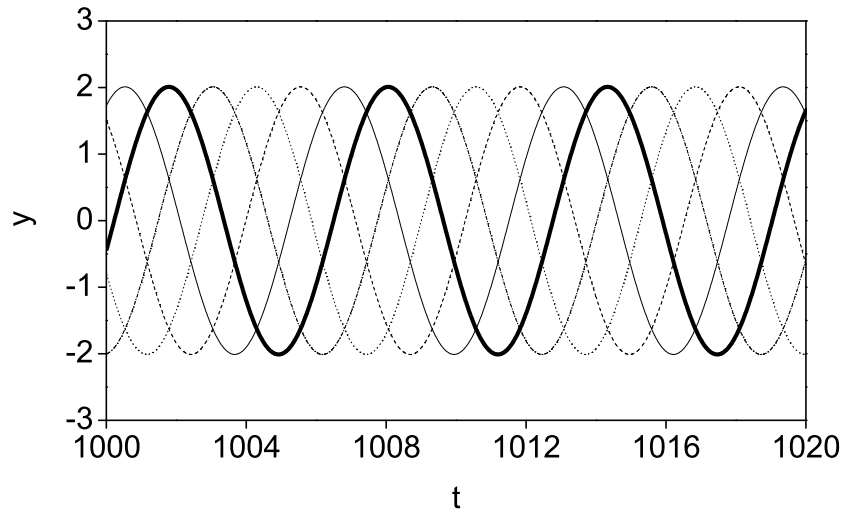


(a)

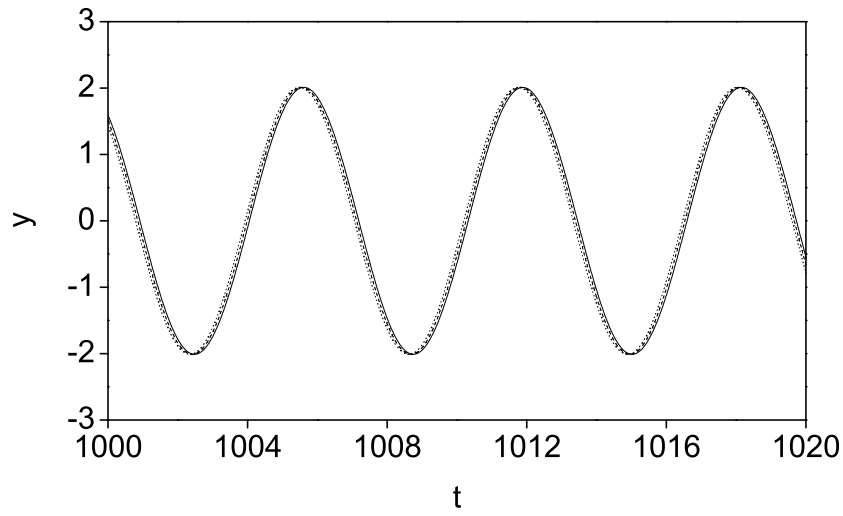


(b)

Figure 6: Time series for $k = 1$. (a) Thick $i = 1$, thin $i = 21$, dashed $i = 41$, dotted $i = 61$, dash-dot $i = 81$. (b) Neighboring oscillators. Lines: solid $i = 40$, dashed $i = 41$, dotted $i = 42$.



(a)



(b)

Figure 7: Time series for $k = -1$. (a) Thick $i = 1$, thin $i = 21$, dashed $i = 41$, dotted $i = 61$, dash-dot $i = 81$. (b) Neighboring oscillators. Lines: solid $i = 40$, dashed $i = 41$, dotted $i = 42$.

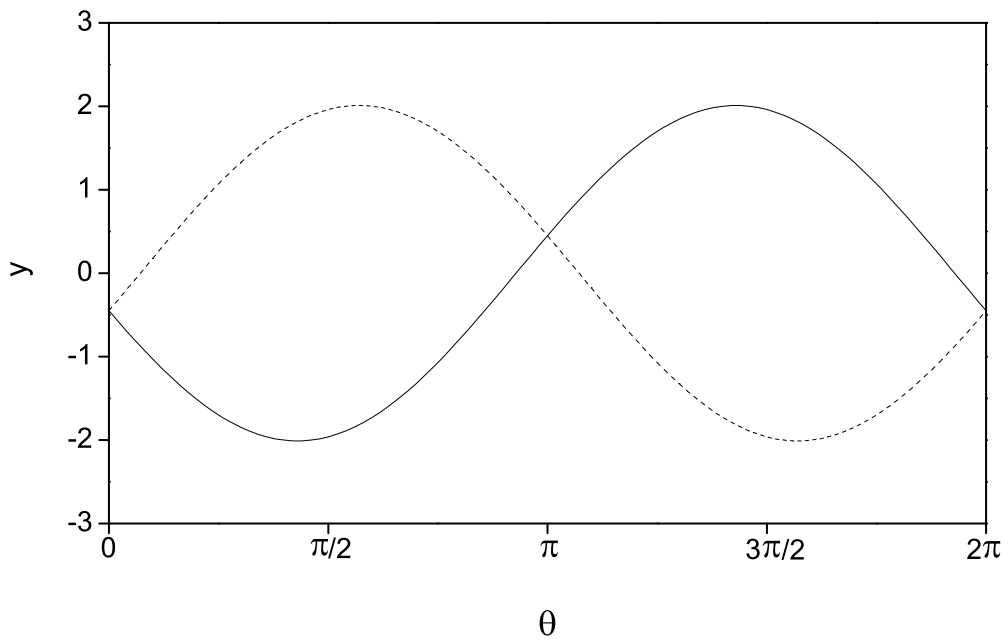


Figure 8: Spatial distribution of y_i at $t = 1000$. Lines: solid $k = 1$, dashed $k = -1$.

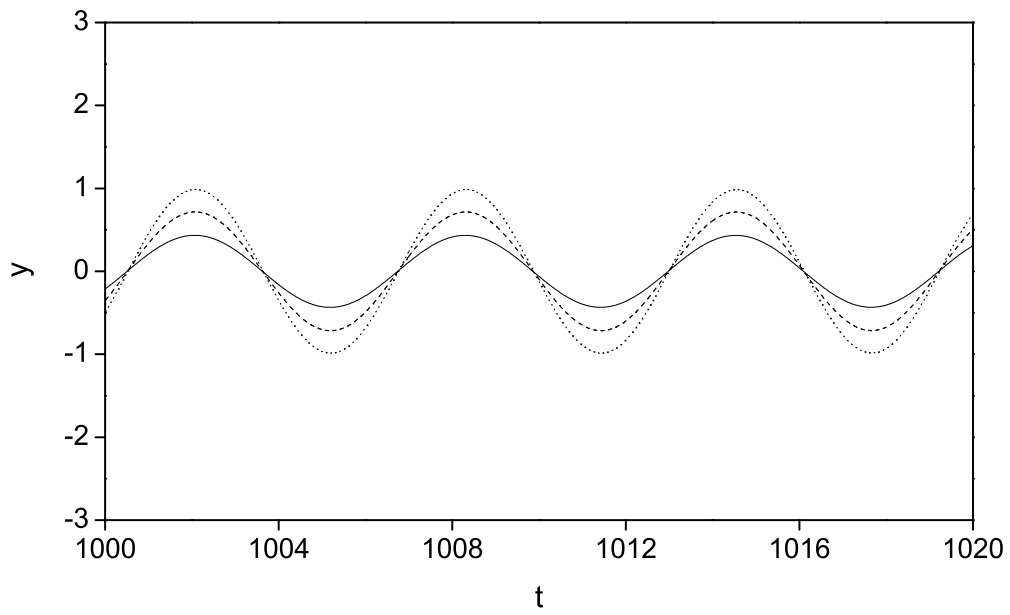
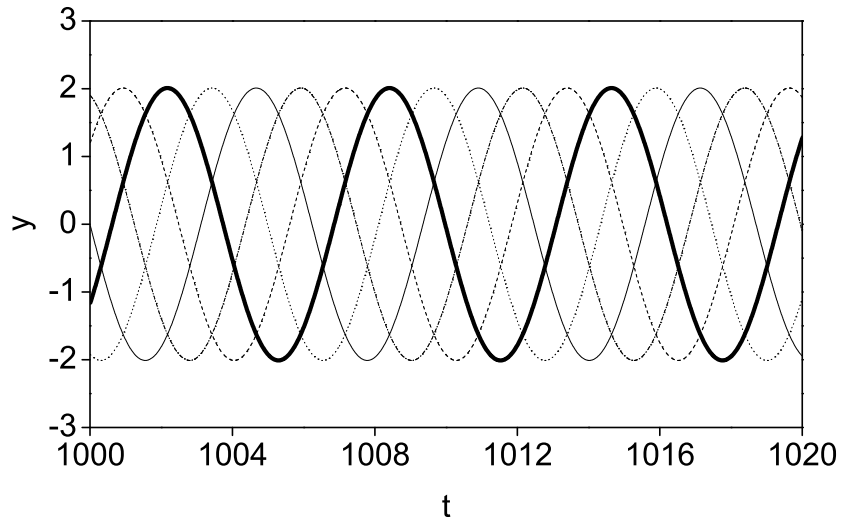
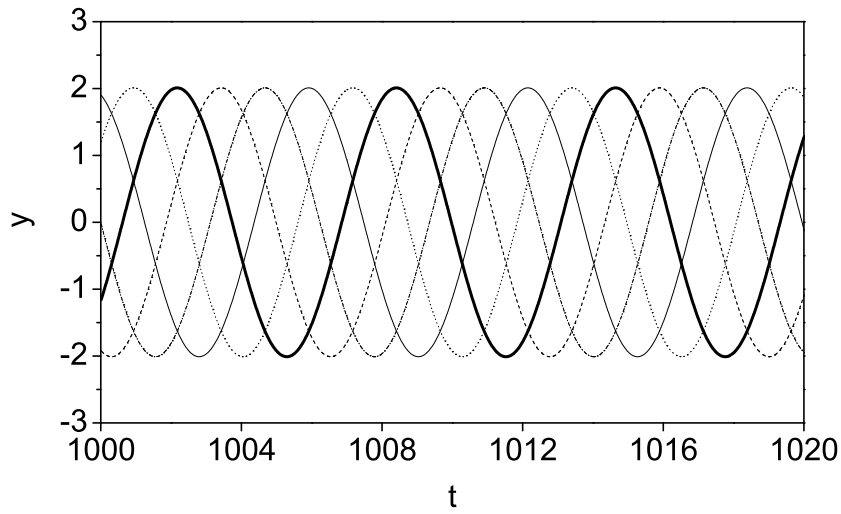


Figure 9: Time series for standing wave with $k = 1$ and neighboring oscillators. Lines: solid $i = 40$; dashed $i = 41$; dotted $i = 42$.



(a)



(b)

Figure 10: (a) Time series for $k = 2$. (b) Time series for $k = -2$. Lines: thick $i = 1$, thin $i = 21$, dashed $i = 41$, dotted $i = 61$, dash-dot $i = 81$.

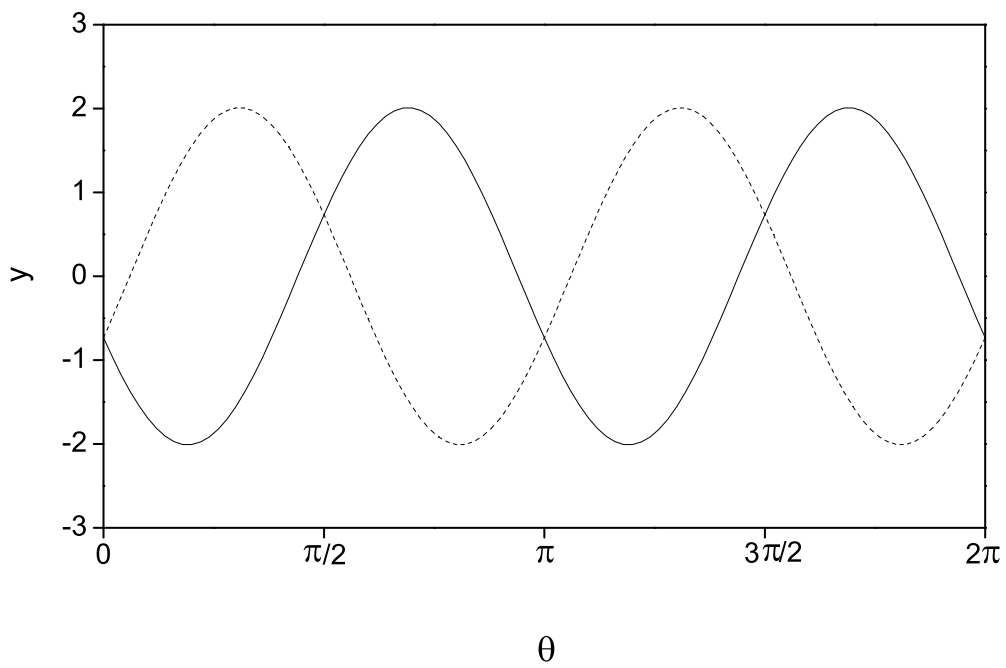
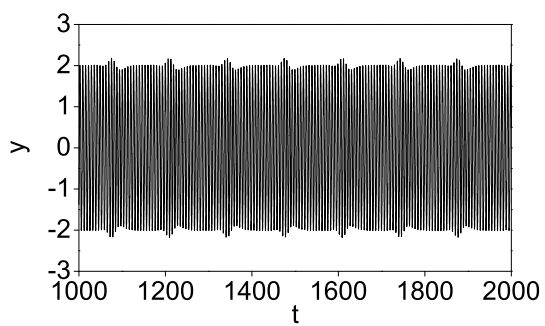
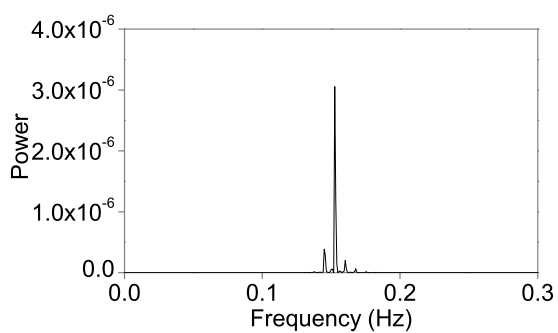


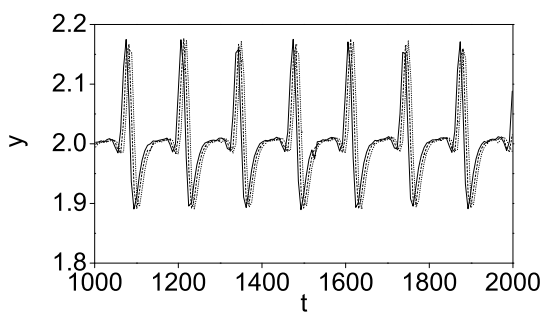
Figure 11: Spatial distribution of y_i at $t = 1000$. Lines: solid $k = 2$, dashed $k = -2$.



(a)

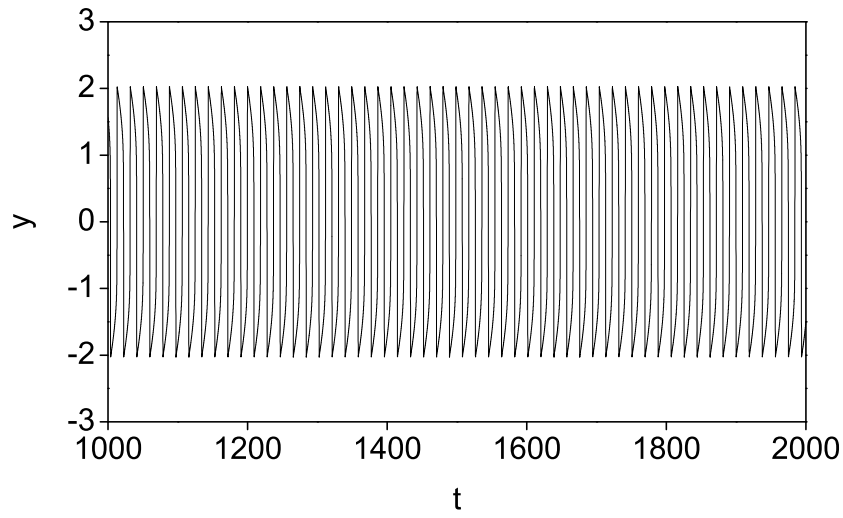


(b)

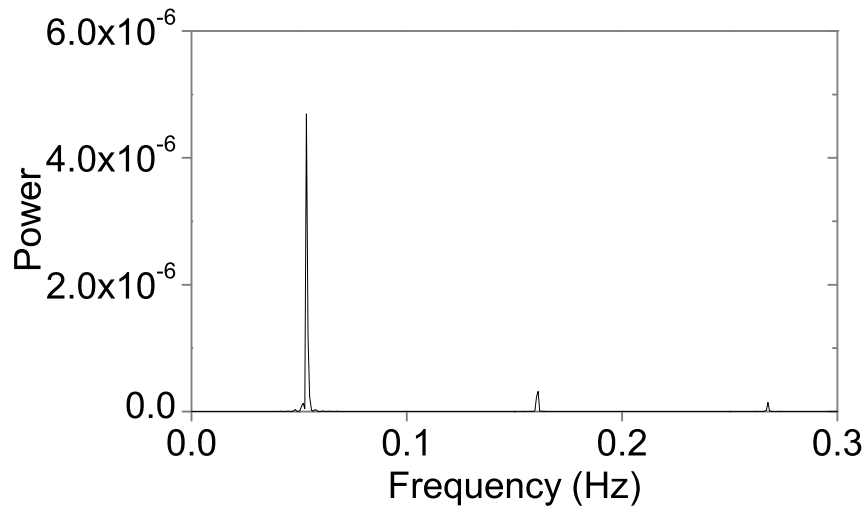


(c)

Figure 12: (a) Time series for $a = 1$, $k = 2$, $i = 1$. (b) Corresponding power spectrum. (c) Detail of envelope to show modulated signal traveling through ring; lines: solid $i = 1$, dashed $i = 2$, dotted $i = 3$.

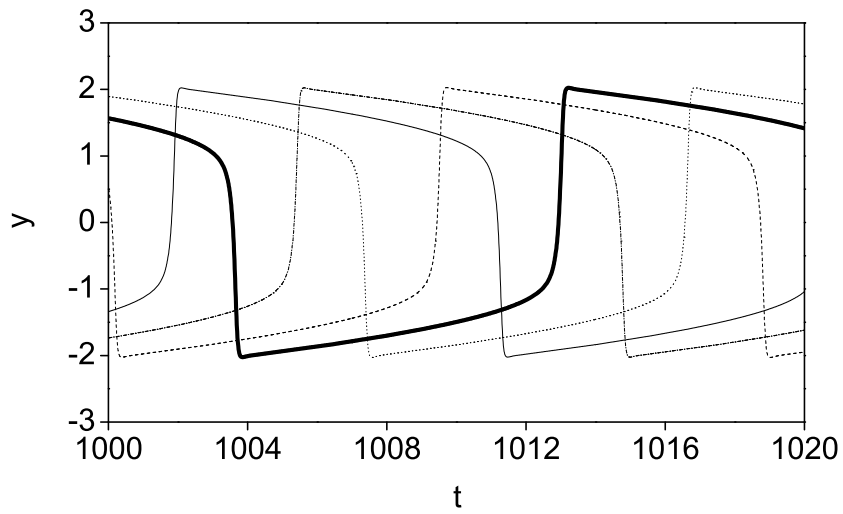


(a)

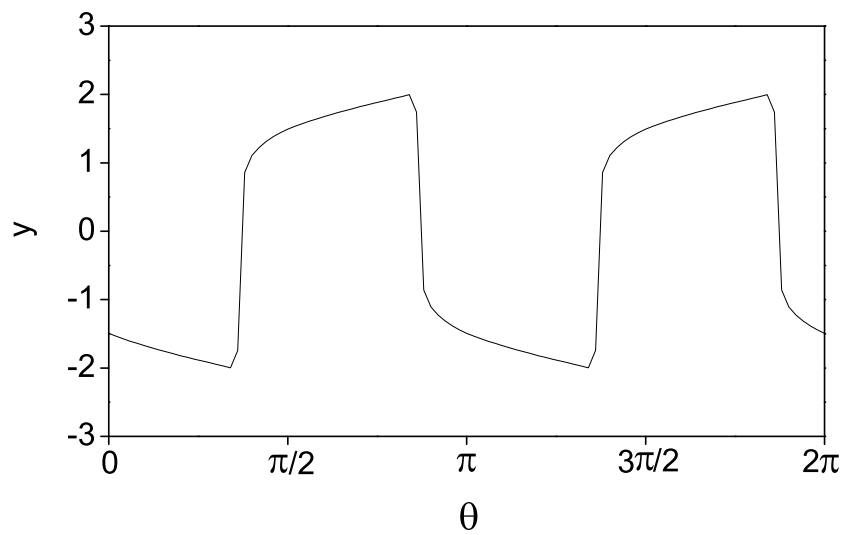


(b)

Figure 13: (a) Time series for $a = 10$, $k = 2$, $i = 1$. (b) Corresponding power spectrum.



(a)



(b)

Figure 14: (a) Time series for $a = 10$, $k = 2$. Lines: thick $i = 1$, thin $i = 21$, dashed $i = 41$, dotted $i = 61$, dash-dot $i = 81$. (b) Spatial distribution of y_i at $t = 1000$.